DOI 10.2478/ama-2024-0035

EXPERIMENTAL AND ANALYTICAL APPROACHES ON AIR SPRING ABSORBERS MADE OF LDPE POLYMER

Maciej OBST*, Dariusz KURPISZ*, Michał JAKUBOWSKI**

*Institute of Applied Mechanics, Poznań University of Technology, ul. Jana Pawła II 24, 60-965 Poznań, Poland
**Faculty of Mechanical Engineering, Poznań University of Technology, ul. Jana Pawła II 24, 60-965 Poznań, Poland

maciej.obst@put.poznan.pl, dariusz.kurpisz@put.poznan.pl, michal.g.jakubowski@student.put.poznan.pl

received 28 April 2023, revised 08 October 2023, accepted 14 October 2023

Abstract: Damping and energy-consuming elements can be found in many technical applications. This means these component types can prevent fractures or injuries in the case of products or people, respectively. In the last time, many modern applications and inventions associated with the reduction of the effects of an impact are observed especially in the mode of transportation safety area. The significant development of the automotive industry, increasing popularity of motorbikes, electric bikes and scooters, sports field, etc., require new solutions for personal safety protection. Human head and neck protection, and other body parts protection are typical groups of solutions from biomechanics and mechanical engineering. Authors have investigated LDPE-made pneumatic absorbers under axial impact force. Based on the experimental approach and analytical model, mechanical characteristics are presented. Impact force value, deceleration and damping for different loading conditions are shown. Because safety systems' impact protective features can be matched to impact conditions, results indicated that absorber damping could possibly be a good solution for them, shaping the impact characteristics according to safety requirements.

Key words: LDPE absorbers, reaction on impact, analytical approach, mechanical parameters, impact test, LDPE bellows impact, protective

1. INTRODUCTION

Materials, components or structures are very often subjected to complex loading covering a dynamic one. This means the stress state is represented by a few components, and deformation can occur at more complicated features than it can be noticed at a one-axial loading type (1,2). Research on the dynamics behaviour of materials and structures can be divided into experimental researches (3–8), simulation ones and hybrid methods (9–12). Modern materials and rapid development of engineering materials create new opportunities for scientists and engineers dealing with the protection of human health and life. Dynamic tests concerning the loading impulse are the basis for all activities aimed at developing more and more effective protection systems against the effects of accidents. The review paper (13) contains a list of currently designed layered structures acting as impact and explosion energy absorbers. Attention was drawn to the enormity of works related to the dynamic study of layered structures, which makes the topic up-to-date due to the attempt to unify the issue. The structures of the cores are interesting because they are designed based on origami inspiration. Structures with auxetic properties are also geometrically complex and give possibilities of impact energy-absorbing applications. Interest in auxetics as cores of layered energy-absorbing structures is a very interesting direction. In this paper, a layered structure was also specified, where the core is made of pipes arranged parallel to each other, perpendicular to the linings. Attention is paid to the material from which pipe cores are currently made. They are metals or polymers. Tubes filled with foam are characterised by very good energy consumption. Structures of this type are used in protection against the effects of impacts at relatively low speeds, where structure performance may occur. In paper (3), the method of dynamic testing of polypropylene obtained uniaxial effects, determining the strain rate values at the following levels: 100 s^{-1}, 200 s^{-1}, 300 s^{-1}, 400 s^{-1} and 500 s^{-1} was presented. During the experiment, the authors have used a split-Hopkinson pressure bar giving constant strain rates. The obtained results of dynamic tests were compared with the quasi-static test ones. Lower values of strain at destruction at dynamic loading were observed. In the analysis of the results, the wave phenomenon was taken into account, based on the one-dimensional wave theory. Jordan et al. (4) also used the split-Hopkinson pressure bar and the relationship between strain rate and grain size and mechanical properties of OFHC copper was investigated. The measurement of the radial and longitudinal deformation was carried out using the laser technique together with the registration of images with a high-speed camera. It was pointed out that the Poisson ratio in dynamic tests assumes a constant (14). The results of tension dynamic tests of X20MnAlSi16-3-3 steel are presented. A rotary hammer was used, which allows setting the strain velocity in the range 5–40 m/s. Based on the obtained results, it was found that the tested high-grade steel strengthens with increasing strain velocity values. An increase in the hardness of the tested steel was observed (5). Experimental and analytical results for a radially loaded ring during an explosion are presented. Ring deformations were measured using the X-ray method. Ring specimens, placed on a cylindrical explosive charge, made it possible to measure changes in radius and deformation rate. In theoretical investigations, the

specimen ring was treated as a thin-walled structure, assuming: symmetry during sample deformation, plane strain state occurrence, ring outer side pressure equal to zero, isotropic properties, no compressible, ideal plastic material and the instantaneous value of the ring sample radius is determined experimentally. Analytical model of investigated ring was based on the Tresca condition. Stankiewicz et al. (15) presented the results of energy consumption tests of the following elastomers: Asmathane (65 ShA), Asmaprene BE (55 ShA), Asmaprene Q (55 ShA), Easyprene FPS (30 ShA), Biresin U1303 (hardener Biresin U1402), Biresin U1305 (hardener Biresin U1305) and Biresin U1419 (hardener Biresin U1419). Properties of these materials are resistance to large deformations and thermal dissipation of impact energy. A drop tower was used as a test stand, where piezoelectric force sensor and laser displacement sensor was applied. In the study, a high-speed camera was used to record successive cycles of dynamic specimen deformations. The authors based on the obtained experimental characteristics, build constitutive models of dynamic mechanical material properties. Then, models were applied to numerical investigations and design impact protection cover. In paper (11), Raponi and Fiumarella presented experimental and numerical analysis of attenuator made of thermoplastic composite material parameter identification under axial impact loading. Composite materials have light weight and good energy dissipation. Investigated truncated-cone shape bumper with a rectangular cross-section was crushed in a quasi-static experimental test. Kathiresan et al. (12) described results of the experimental and simulation of quasi-static compression test of thin-walled cone made of glass fibre and epoxy resin reinforced composite. Conical specimens had different forming angles. Loading deformation characteristics were compared with those obtained by Abaqus simulation. In paper (16), new proposition of glass or carbon fibre sandwich panel with foam core was presented. Prepared panels was tested for impact load under different energy. Authors used Instron Dynatup 9250HV drop weight impact testing machine and did tests according to the ASTM norm. Applied impact head speed was equal to 2 mm/min. Avalle Belingardi (17) presented a model of the foam material, the purpose and application of it which is to give possibilities to select the appropriate foam due to the absorption of impact energy. The presented model of the foam material includes, among others, the influence of the strain rate on its mechanical properties. Proposed foam one-dimensional material model is fitted to experimental data based on past experimental data of the authors. The aluminium foam model studies included quasi-static, dynamic, and impact tests at different loading speeds and impact energy. It was pointed out that foams are materials commonly used in devices protecting the safety of people and in the transport of delicate goods. In paper (9), Koohbor et al. presented the results of mechanical energy absorption tests under low-velocity impact loading for elastomeric hybrid structure polyurethane foam. The authors pointed out on the measure stress and strain in foam structure, energy indicators and evolution of the Poisson ratio. Optical systems were used during experimental tests. The examined foam behaviour was characterised by an increase of strength value when strain rate increased. Reyes and Børvik (8) presented the continuation of their research on the energy dissipation properties of layered structures. Various foams acting as the core were tested. Thin aluminium plates were used as covers. Dynamic loading was used by means of the drop tower, where a constant mass of 15 kg impacted the tested specimens with different velocities between 5 m/s and 10 m/s. During the research, high-speed cameras were used to record the movement. In conclusion, it was found that the best energy dissipation effects can be obtained by using low-density foam cores. In paper (18), foam-filled, thin-walled structures were presented as mechanical energy absorbers. The interesting fact is that foam density varies throughout the foam depth. The authors noted that variable foam density has a significant influence on the energy dissipation process during impact. Investigated structures were prepared as square, thin-walled aluminium-made pipes filled by aluminium foam, where foam density varies on the specimen length in accordance with impact direction. Research was made by the FEM simulation software. Robinson et al. (19) investigated the interaction between head and protective football helmet under impact load. Influence factors that lead to mild traumatic brain injury (MTBI) were the main revealing goal of the researchers. The authors pointed out that the reduction of the coefficient of friction between the head and the helmet liner results in a reduction of overloads acting on the head. In paper (20), Maw et al. investigated skater's helmets under impact loading, where helmet size and shape were decision-making parameters. During the experimental tests, the helmet fell on the special pad. The authors used four levels of the drop. As a conclusion, it was found that the size and the helmets' radius of curvature have an important influence on the linear decelerations during the helmet impact. Research on the energy consumption of helmets is also presented by Clough et al. (6). Modern elastomeric lattice properties, applied as helmet shock absorber padding are investigated. The researchers have paid attention to two types of materials used as helmet linings: single-hit material and self-recovering. Resistance to multiple impacts undoubtedly increases the usefulness of the helmet. Additive manufacturing of cellular architecture is giving new possibilities to design more effective cellular structure where we can design more precisely the safety properties. The problem of head overloads was studied by Lewis et al. (21), where they experimentally investigated the problem of head acceleration, which was protected by football helmets. Volunteers between the age of 16 years and 30 years, with football helmet worn, had accelerometers inside their mouths. They also applied accelerometers installed inside the lining layer. Human cadaver heads were used with and without protective helmets for a more intense impact during tests. In the case of a corpse, blunt impact force was realised by pendulum device. The recorded results were compared with each other, paying attention to the acceleration peak values. The test results showed the advantages of safety helmets. Attention was focussed on the differences between the results of the measured accelerations for the sensors placed in the mouth and the helmet lining. The results of research on the chin part of the full-face helmet were presented by Whyte et al. (22). The finite element method was used for dynamic simulation of the helmet behaviour. The author applied two composite layers to increase the stiffness of the chin part of the helmet. This modification resulted in a reduction of peak acceleration of the head. It was noted that the stiffness of the foam lining the helmet should be selected in correlation with the properties of the helmet shell. The lowest acceleration values were obtained when the stiffness of the helmet shell was increased and the stiffness of the foam lining inside the helmet was reduced. Trzaskalska and Chwastek (7) conducted studies on the effect of the density of ski helmet liners made of expanded polystyrene (EPS) in order to assess the energy dissipation properties. It was found that increasing the EPS density increases the damping properties while reducing flexibility and increasing the hardness and brittleness of the ski helmet

DOI 10.2478/ama-2024-0035

liners. Mizuno et al. (10) used FEM simulations for the investigation of cyclist helmet properties protection during the impact of vehicle A-pillar. Due to the high stiffness of the A-pillar, a head impact results in serious injuries. It was noted that, in the case under study, the helmet liner had little effect on the HIC parameter but by reducing the stiffness of the A-pillar, the HIC parameter can be reduced. It should be noted that the authors used a simplified FEM simulation model. Considerations led by Ghajari et al. (23) made it possible to notice that the tests of protective helmets are carried out using standard heads, ignoring the rest of the body. Using the finite element method, a full-face helmet study was conducted taking into account the interaction of the whole body during impacts. The authors pointed out that even during 10 m/s impact, the whole body causes the helmet liner to be crushed. The results described by Wu et al. (24) present the resistance to the secondary impacts of construction helmets. It was found that the protective performance of these helmets can be improved by using polyethylene air-bubble cushions. During the experimental tests, a drop tower was used. Multiple strokes were performed at different times by dropping the impactor with an accelerometer from different heights. The authors found that the use of air-bubble cushions significantly improves the protective qualities of construction helmets. Mazurek and Szyguła (25) performed a numerical FEM analysis of the impact on a thin-walled aluminium-made column. Columns with circular, square and triangular cross-sections were tested at the impact velocity of 30 km/h. The influence of notches on the crushing process of the columns was also examined. Based on the research, interesting conclusions were drawn. During axial impact, the cross-sectional shape of the column affects the dissipated energy capacity. The columns with notches or embossing results in increase of the amount of dissipated energy and a more favourable deceleration curve. Research results are presented in Böhm et al. (26) for conducted tests on the front bumper bracket of a passenger car. Bumper bracket was made from carbon fibre epoxy bumper brackets reinforced with 2D biaxial and 2D triaxial braids. Experimental studies were conducted on a dedicated drop tower equipped with fast cameras. Simultaneously, numerical research was carried out in the Abaqus software. The usefulness of new phenomenological textile-reinforced composites models of all damages were also demonstrated. Raponi and Fiumarella (11) presented the results of experimental and simulation tests of a bumper made of thermoplastic composite. Material parameters were identified on the basis of the experimental study. The crushing test of the component was performed and compared with the results of the computer simulation. Optimisation of the simulation model was carried out by adapting it to the characteristics of the load-displacement based on the experimental crushing test.

In the current paper, the results of selected experimental and analytical approaches for the air LDPE absorbers system will be presented. The attention follows not only the influence of impact velocity on mechanical characteristics, but is focussed on analytical description of the relation between dynamic characteristics for open and closed LDPE absorbers system.

2. EXPERIMENTAL IMPACT TESTS

Laboratory tests were carried out using a drop tower stand with a steel 0.2-kg mass impactor. The free fall of the impactor took place from several levels relative to the base of the test stand, namely: 200 mm, 400 mm, 600 mm and 900 mm. During the impact test, the impactor hit the aluminium plate bumper shown in Fig. 1, equipped with very low friction coefficient ball bearings, one in each corner. The aluminium plate bumper moved along the corner bar guides, where the resistance to movement was negligible. Pneumatic LDPE absorbers have been impact loaded, where at the same time, four spring LDPE absorbers were tested and placed parallel.

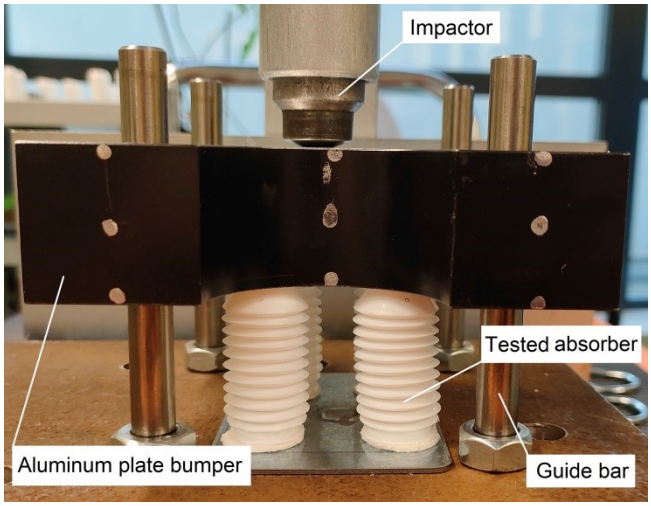

Fig. 1. Impact test stand

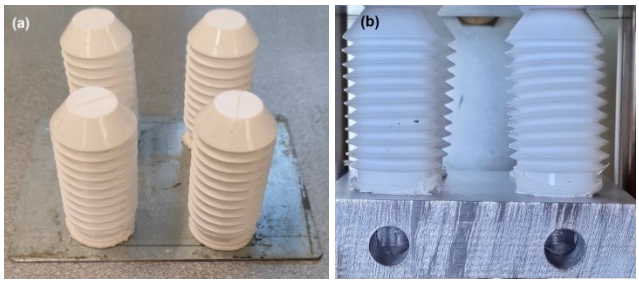

Fig. 2. Pneumatic LDPE absorbers: (a) sealed absorbers, (b) free airflow absorbers

Tested LDPE absorbers were examined as sealed space—Fig. 1, where the air was compressed under impact loading, and in another case, when free airflow was released through a passage channel in the steel base of the absorber—Fig. 2b. In the second case, only the dynamic stiffness of the LDPE absorber was followed. The results of the experimental research were dynamic characteristics for the air-compressing absorber and the absorber with the resistance posed only by its shell.

3. LDPE FOIL TENSION TEST RESULTS

LDPE polymer used to produce the tested absorbers was delivered in a sheet of foil form. A specimen was subjected to a static tensile test at room temperature. Based on results from the tensile test, fundamental LDPE mechanical characteristics were elaborated—Fig. 3.2.

Fig. 3.1. Specimen of LDPE foil used in the tensile test

The thickness of the foil sheet wasn't constant and it oscillated from 0.36 mm to 0.39 mm.

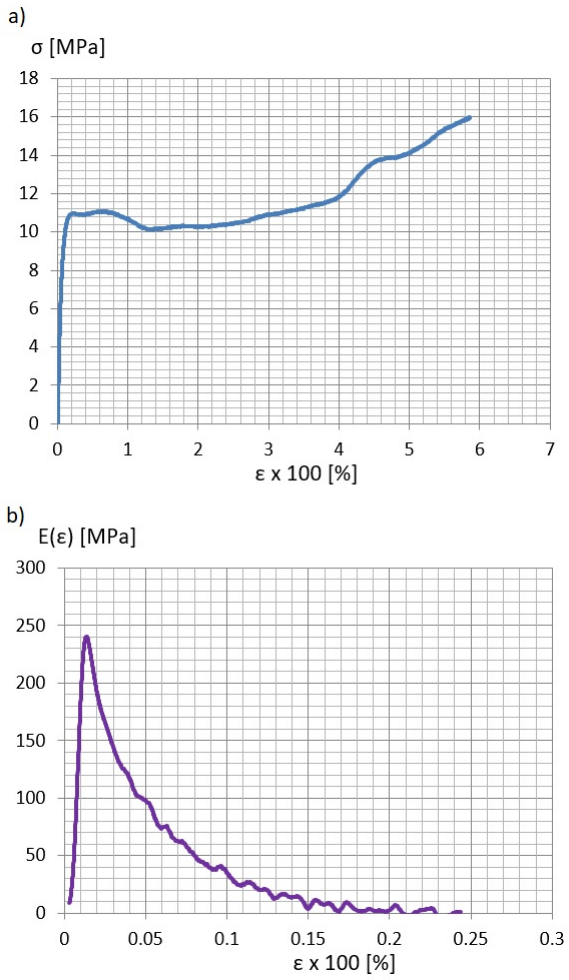

Fig. 3.2. Stress–strain relations (a) for tangential modulus E(ε) (b) for LDPE

4. ANALYTICAL MODEL OF PNEUMATIC ABSORBER

Based on the experimental dynamic results of the LDPE absorbers, a phenomenological analytical description was proposed. The purpose of the analytical research was focussed on the description of the impact phenomenon.

For the clarity of the investigations, the following assumptions were taken:

- The geometry and the static characteristics of the absorber are well-known.
- The absorber's deflection was connected only with the reaction of its harmonic part.
- The absorber was filled with the medium (air) about the initial pressure, p_o [MPa] and the temperature compatible with the ambient temperature.
- The connection between the absorber and the base is perfectly tight.
- Impact time is so short that every exchange of the thermal energy with the ambient does not exist.

Due to the complete tightness of the discussed absorber and its volume change as a consequence of dynamic compression, the relation between current values of pressure, p, and volume, ϑ [mm^3], is the same, like in the case of adiabatic transformation. In consequence, we can write:

$$p\vartheta^{\kappa} = const. \tag{4.1}$$

where κ is the Poisson's coefficient, depending on the medium fitting the absorber.

Therefore, for the increase of pressure, Δp, caused by the volume change, $\Delta\vartheta$, the following relationship is true:

$$p_o\vartheta_o^{\kappa} = (p_o + \Delta p)(\vartheta_o + \Delta\vartheta)^{\kappa}, \tag{4.2}$$

and hence:

$$\Delta p = p_o \cdot \left[\left(\frac{\vartheta_o}{\vartheta_o+\Delta\vartheta}\right)^{\kappa} - 1\right], \tag{4.3}$$

or equivalently:

$$\Delta p = p_o \cdot \left[\left(1+\frac{\Delta\vartheta}{\vartheta_o}\right)^{-\kappa} - 1\right], \tag{4.4}$$

where p_o and ϑ_o are respectively the initial values of pressure and absorber's volume.

According to Pascal's law, because the pressure propagates independently in the direction, it can be considered that it is the quotient of the force increment, ΔF_1 [N], (of the gas pressure) and the cross-surface area, A_o [mm^2], of the absorber, which in effect gives:

$$\Delta F_1 = A_o p_o \cdot \left[\left(1+\frac{\Delta\vartheta}{\vartheta_o}\right)^{-\kappa} - 1\right], \tag{4.5}$$

where $A_o = \frac{1}{4}\pi D^2$ and D are absorber's cross-section diameter.

In order to determine the initial volume, ϑ_o, and its change, $\Delta\vartheta$, let's consider the absorber geometry, based on Fig. 4.1.

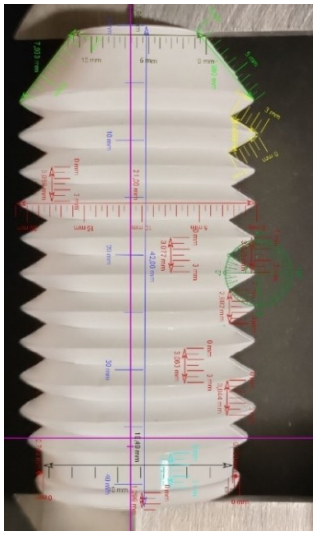

Fig. 4.1. Detail dimensions of the discussed absorber

DOI 10.2478/ama-2024-0035

Based on the measurements, the work of the spring absorber can be illustrated, just like in the following figures.

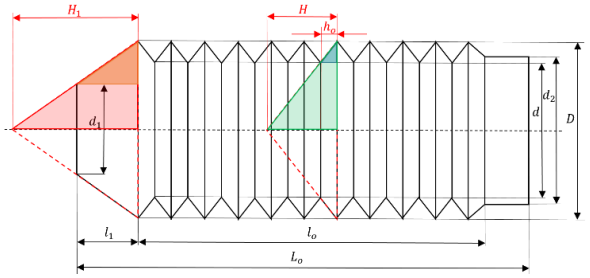

Fig. 4.2. Absorber geometry parameters in the initial state

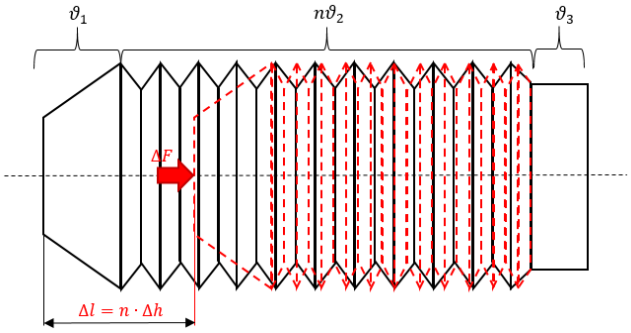

Fig. 4.3. Deflection of the absorber

Assuming the acceptable simplification of the shape, geometry can be assumed that the initial volume of the absorber is:

$$\vartheta_o = \vartheta_1 + n\vartheta_2 + \vartheta_3, \tag{4.6}$$

where ϑ_1, ϑ_2 and ϑ_3 denote the volume of the top, working and base parts of the absorber, respectively.

The similarity between two pairs of triangles: orange and red, blue and green implies:

$$H_1 = \frac{D}{D-d_1} \cdot l_1, \tag{4.7}$$

and

$$H = \frac{D}{D-d} \cdot h_o, \tag{4.8}$$

which gives:

$$\vartheta_1 = \frac{1}{12}\pi D^2 H_1 - \frac{1}{12}\pi d_1^2 (H_1 - l_1) = \frac{1}{12}\pi[(D^2 - d_1^2)H_1 + d_1^2 l_1] = \frac{1}{12}\pi(D^2 + Dd_1 + d_1^2)l_1, \tag{4.9}$$

$$\vartheta_2 = \frac{1}{12}\pi D^2 H - \frac{1}{12}\pi d^2 (H - h_o) = \frac{1}{12}\pi[(D^2 - d^2)H + d^2 h_o] = \frac{1}{12}\pi(D^2 + Dd + d^2)h_o. \tag{4.10}$$

Using Eq. (4.6), we get:

$$\vartheta_o = \frac{1}{12}\pi(D^2 + Dd_1 + d_1^2)l_1 + \frac{1}{12}\pi n(D^2 + Dd + d^2)h_o + \frac{1}{4}\pi d_2^2(L_o - l_o - l_1). \tag{4.11}$$

According to the interpretation illustrated in Fig. 4.3, the absorber volume change, $\Delta\vartheta$, can be expressed as:

$$\Delta\vartheta = \vartheta - \vartheta_o \tag{4.12}$$

where,

$$\vartheta = \frac{1}{12}\pi(D^2 + Dd_1 + d_1^2)l_1 + \frac{1}{12}\pi n(D^2 + Dd + d^2)(h_o + \Delta h) + \frac{1}{4}\pi d_2^2(L_o - l_o - l_1), \tag{4.13}$$

which gives:

$$\Delta\vartheta = \frac{1}{12}\pi n(D^2 + Dd + d^2)\Delta h. \tag{4.14}$$

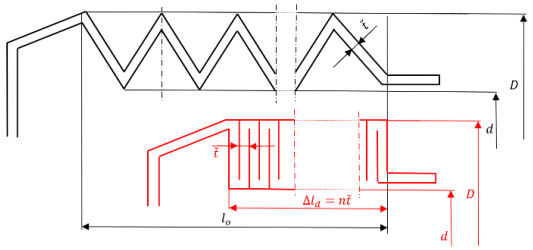

Fig. 4.4. Absorber reaction on compression force

Due to the thickness, $\tilde{t}$, of the absorber surface, elastic compression ends; when its value equals the limit value, $\Delta l_d = n\tilde{t}$ (see Fig. 4.4), which implies the real change of the volume:

$$\Delta\vartheta_r = \frac{1}{12}\pi n(D^2 + Dd + d^2)h_o - \frac{1}{4}\pi d^2(l_o - \Delta l_d). \tag{4.15}$$

On the other hand, based on Eq. (4.14), this reaction implies the volume decrease:

$$\Delta\vartheta_d = \frac{1}{12}\pi(D^2 + Dd + d^2)\Delta l_d. \tag{4.16}$$

During the compensation, the absorber thickness changes its volume, therefore, we introduce the correction coefficient:

$$k = \frac{\Delta\vartheta_r}{\Delta\vartheta_d} = \frac{l_o}{\Delta l_d} - 3 \cdot \frac{d^2}{D^2+Dd+d^2} \cdot \frac{l_o - \Delta l_d}{\Delta l_d}. \tag{4.17}$$

hence:

$$\Delta\tilde{\vartheta} = k \cdot \Delta\vartheta = \frac{1}{12}\pi kn(D^2 + Dd + d^2)\Delta h, \tag{4.18}$$

and next, after substituting into Eq. (4.5), we get:

$$\Delta F_1 = A_o p_o \cdot \left[\left(1 + \frac{nk(D^2+Dd+d^2)\Delta h}{(D^2+Dd_1+d_1^2)l_1 + n(D^2+Dd+d^2)h_o + 3d_2^2(L_o - l_o - l_1)}\right)^{-\kappa} - 1\right]. \tag{4.19}$$

Due to the fact that the complete change of the absorber height, $\Delta l = n\Delta h$ (where, $n\Delta h \leq \Delta l_d$), we can write:

$$\Delta F_1 = A_o p_o \cdot \left[\left(1 + \frac{k(D^2+Dd+d^2)\Delta l}{(D^2+Dd_1+d_1^2)l_1 + n(D^2+Dd+d^2)h_o + 3d_2^2(L_o - l_o - l_1)}\right)^{-\kappa} - 1\right] \tag{4.20}$$

and taking into account the experimental dynamic absorber axial stiffness, C_m (which is known from the experimental results for open LDPE absorbers system), we have:

$$\Delta F_2 = C_m \cdot \Delta l, \tag{4.21}$$

which finally gives:

$$\Delta F(\Delta l) = \Delta F_1 + \Delta F_2. \tag{4.22}$$

The received pattern is an analytical description of the theoretical characteristic of the ideal sealed absorber.

Replacing the absorber height change, Δl, with the displacement, x, along its axis, the equation of motion for a package consisting of N absorber (in our case, $N = 4$) can be written as:

$$m\frac{d^2x}{dt^2} = -N\Delta F(x), \tag{4.23}$$

where m is the running mass.
Because:

$$\frac{d^2x}{dt^2} = V\frac{dV}{dx}, \tag{4.24}$$

so:

$$mV\frac{dV}{dx} = -NA_o p_o \cdot [(1 - Bx)^{-\kappa} - 1] - NC_m x, \tag{4.25}$$

where:

$$B = \frac{k(D^2+Dd+d^2)}{(D^2+Dd_1+d_1^2)l_1+n(D^2+Dd+d^2)h_o+3d_2^2(L_o-l_o-l_1)}. \tag{4.26}$$

Finally, using of condition, $V(0) = V_o$, it can be written that:

$$V = \sqrt{V_o^2 + 2N\frac{A_o p_o}{Bm}\cdot\left\{\frac{1}{1-\kappa}[(1-Bx)^{-\kappa+1} - 1] + Bx\right\} - N\cdot\frac{1}{m}C_m x^2}\,. \tag{4.27}$$

Returning to the substitution, $V = \frac{dx}{dt}$, the relation between compression, x, and time, t, can be expressed as:

$$t = \int_0^x \frac{dx}{\sqrt{V_o^2+2N\frac{A_o p_o}{Bm}\cdot\left\{\frac{1}{1-\kappa}[(1-Bx)^{-\kappa+1}-1]+Bx\right\}-N\cdot\frac{1}{m}C_m x^2}}. \tag{4.28}$$

Based on the above equation, it is possible to determine the relation between the dynamic absorbers deflection and time in the case of an ideal sealed system of absorbers, on the base of the same characteristic but in the free flow of air state. The determined characteristics are presented and discussed in the next part of the current paper.

5. APPROXIMATION OF EXPERIMENTAL RESULTS AND APPLICATION OF THEORETICAL INVESTIGATIONS

The basic experimental characteristic was the relation between deflection, x, of the LDPE absorbers system, and the time, t, (see blue lines in Fig. 5.1). The necessity of the achievement of the calculated values of velocity $V(t)$, acceleration $a(t)$ and force $F(t)$ implies that the approximation $x(t)$ should be three times differentiable and equal zero at zero point $(x(0) = 0)$.

To achieve the above assumptions, the approximation function was taken in the form:

$$x(t) = a \cdot \sin(bt) \quad \text{for } t\,\langle 0; \frac{\pi}{2b}\rangle\,, \tag{5.1}$$

and in consequence:

$$V(t) = \dot{x}(t) = ab\cos(bt) \text{ for } t\,\langle 0; \frac{\pi}{2b}\rangle, \tag{5.2}$$

$$a(t) = \dot{V}(t) = -ab^2\sin(bt) = -b^2x(t) \quad \text{for } t\,\langle 0; \frac{\pi}{2b}\rangle, \tag{5.3}$$

$$F(t) = m_P \cdot a(t) = -m_P \cdot b^2 x(t) \text{ for } t\,\langle 0; \frac{\pi}{2b}\rangle, \tag{5.4}$$

and finally:

$$\dot{F}(t) = -m_P \cdot b^2\dot{x}(t) = -m_P \cdot ab^3\cos(bt), \tag{5.5}$$

where a and b are experimental coefficients and m_P is the mass of the palte.

It is easy to see that:

$$F(t) = -m_P \cdot b^2 x(t) = -C_p x(t), \tag{5.6}$$

where $C_p = m_P \cdot b^2$ is the experimental dynamic stiffness, and

$$C_m = \frac{1}{N}\cdot C_p, \tag{5.7}$$

is the dynamic stiffness of a single absorber.

The approximations of experimental characteristics is illustrated. Based on the results of the experiments, the initial velocities of the bumper, corresponding to the falls of the impactor from the heights of 200 mm, 400 mm, 600 mm and 900 mm, were assumed to be equal to: 0.66 m/s, 0.93 m/s, 1.15 m/s and 1.33 m/s.

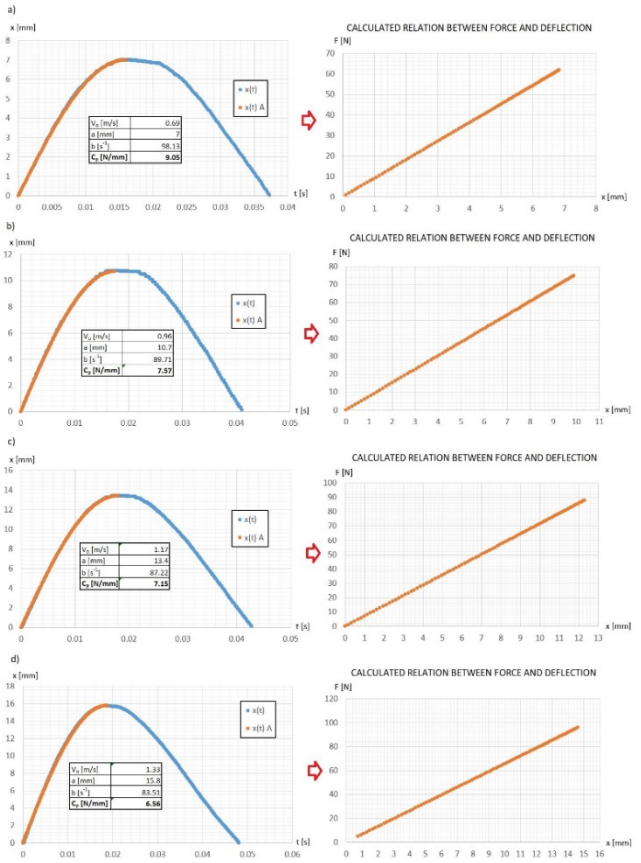

Fig. 5.1. The approximation (orange line) of experimental characteristics (blue line) for open absorbers system in case of initial velocity: (a) $V_o = 0.69\ [\frac{m}{s}]$, (b) $V_o = 0.96\ [\frac{m}{s}]$, (c) $V_o = 1.17\ [\frac{m}{s}]$, (d) $V_o = 1.33\ [\frac{m}{s}]$

Dynamic stiffness of the free flow of the air LDPE absorbers system, determined on the basis of experimental characteristics approximation, at different values of the initial deflection velocity, is presented on the graph (Fig. 5.2).

DOI 10.2478/ama-2024-0035

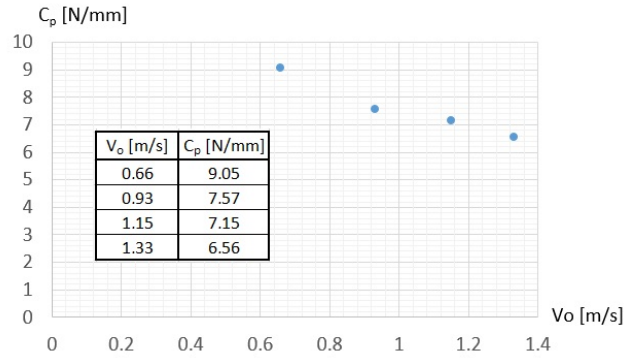

Fig. 5.2. Dynamic stiffness of free flow of air LDPE absorbers system at different values of initial impact velocity

Using the above experimental dynamic stiffness of a free flow of air LDPE absorbers system, one can determine the theoretical characteristic $x(t)$ for a closed system (see Eq. 4.28). With respect to the possibility of validation of the results of theoretical approaches, the experimental characteristics of the closed system were introduced (see Fig. 5.3), while theoretical and experimental characteristics are presented in Fig. 5.4.

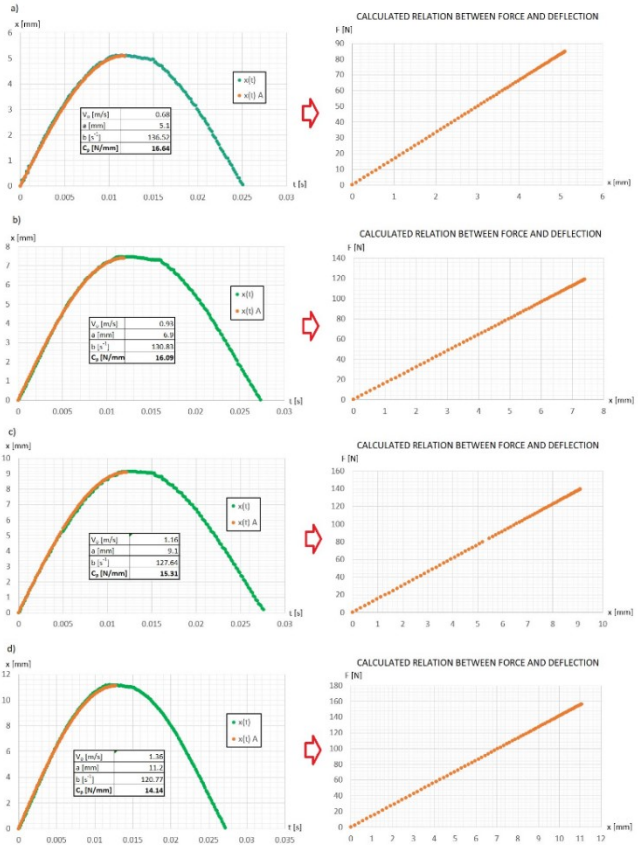

Fig. 5.3. Dynamic stiffness of sealed absorbers system for different value of initial deflection velocity

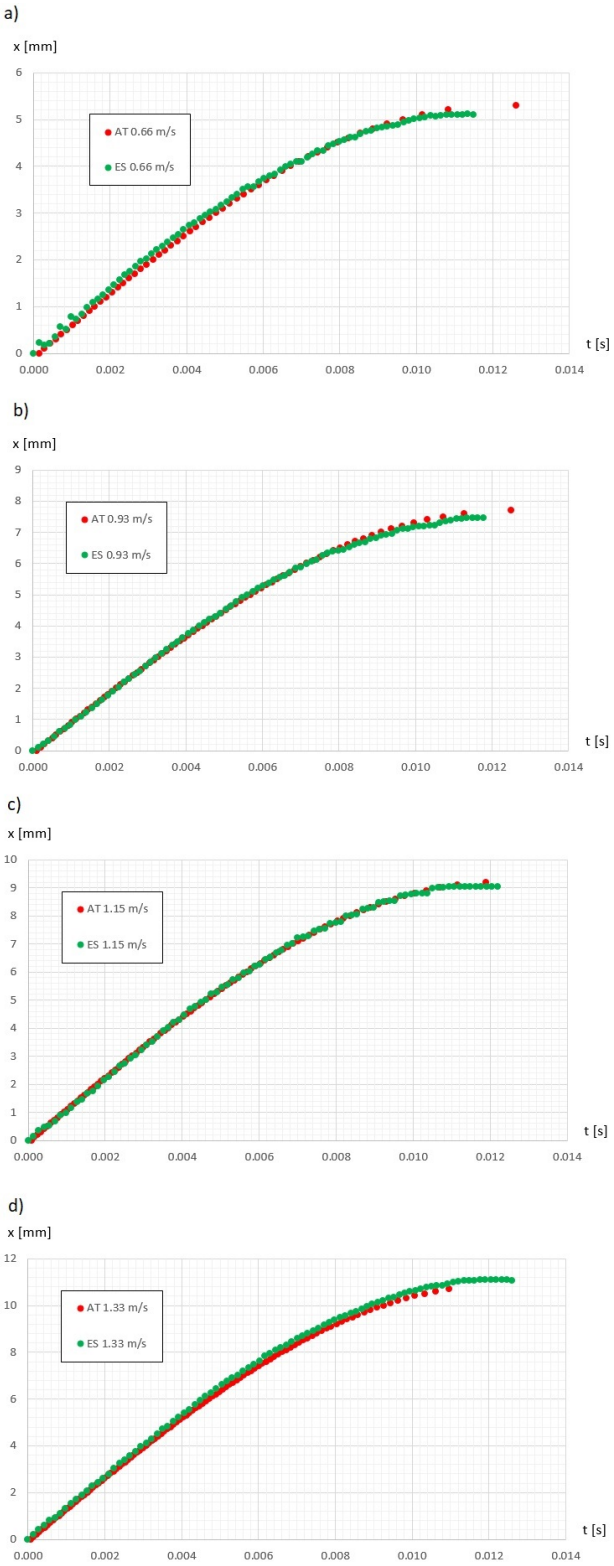

Fig. 5.4. The comparison of the theoretical curve x(t) (red line) on experimental (green line) by initial absorber compression velocity: (a) 0.66 m/s, (b) 0.93 m/s, (c) 1.15 m/s and (d) 1.33 m/s

Using experimental characteristics (see Fig. 5.1), one can define the damping parameter as:

$$T = \left(1 - \frac{E_{k2}}{E_{k1}}\right) \cdot 100\%, \tag{5.8}$$

where E_{k1} and E_{k1} denote, respectively, the kinetic energy of the absorbers system at the beginning and end of the impact test.

Because the energy is a function of mass and current velocity, this can be written in the following form:

$$T = \left(1 - \frac{V_2^2}{V_1^2}\right) \cdot 100\%, \tag{5.9}$$

where V_1 and V_2 are, respectively, the velocity at the beginning and end of the impact process.

The experimental values of damping have been presented in Fig. 5.5.

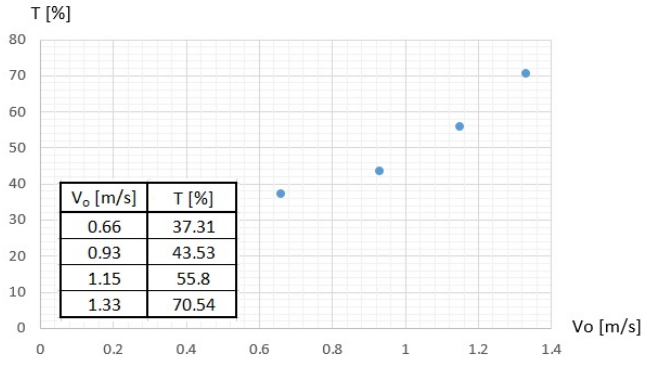

V_o [m/s]	T [%]
0.66	37.31
0.93	43.53
1.15	55.8
1.33	70.54

Fig. 5.5. The values of damping for free flow of air absorbers system

Based on the Eq. (5.5), the intensity of force change can be determined.

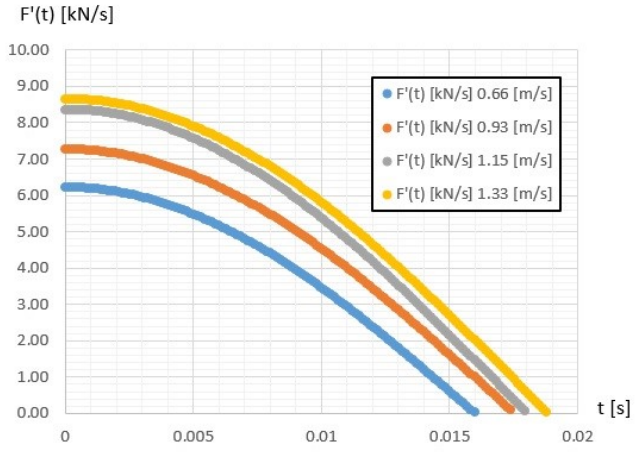

Fig. 5.6. The intensity of change reaction force for the free flow of air absorbers system

6. RESULTS AND DISCUSSIONS

The obtained results of experimental and analytical approaches enabled to notice several interesting aspects of functioning of the LDPE absorbers system. At the beginning, it was easy to observe that the dynamic deflection–time relation is strictly connected with the initial value of deformation velocity. The contraction maximum value of the open absorbers system increases due to the value of initial velocity (see Fig. 5.1), but the stiffness, C_p, decreases (see Figs 5.1 and 5.2).

At bigger numbers of absorbers, the stiffness palte increases while compression decreases their stiffness and decreases the total deflection arrows for the individual initial velocities (see Fig. 5.3). On the ground of adiabatic transformation it is possible to describe the compression–time relation for sealed absorbers system, based only on the same relation for open air LDPE absorbers system (see Eq. 4.28). The agreement between the analytical solution and experimental results is satisfactory (see Fig. 5.4).

The relationship between the damping of the free flow absorbers system and the initial value of deformation velocity is still interesting. The results obtained on the basis of the analysis of experimental characteristics allow us to conclude that the attenuation increases with the increase of the initial strain rate (see Fig. 5.5), that can be connected among others with the mechanical properties of the absorbers construction materials and motion of the air. The air pressure influence of the tight absorbers system stiffness is still an open question, and it will be one of the future aims for the authors' investigations.

7. CONCLUSIONS

Tested, sealed and free airflow absorbers made of polymer LDPE are primarily characterised by usability in the energy-intensive sense. The possibility of estimating the damping values for sealed absorbers compressing air during impact was demonstrated. The characteristics of dynamic properties of the sealed LDPE absorbers at extreme loading conditions were analytically modelled, showing the perfect agreement of the approximation with the results obtained experimentally. It is advisable to conduct further research on the presented absorbers whose dynamic characteristics will be between the extreme cases presented in this paper, i.e. obtained for a sealed absorber and a free airflow absorber.

REFERENCES

1. Kurpisz D, Obst M. The energetic and experimental based approach to description of basic material characteristics and mechanical properties of selected polymers. Journal of Theoretical and Applied Mechanics. 2020;58:183–93.
2. Wegner T, Kurpisz D. An energy-based method in phenomenological description of me-chanical properties of nonlinear material under plane stress. Journal of Theoretical and Applied Mechanics. 2017;55:129–39.
3. Khlif M, Masmoudi N, Bradai C. Polypropylene tensile test under dynamic loading. Journal of KONES Powertrain and Transport. 2014 Dec 28;21(1):131–8.
4. Jordan JL, Siviour CR, Sunny G, Bramlette C, Spowart JE. Strain rate-dependant mechanical properties of OFHC copper. J Mater Sci. 2013 Oct;48(20):7134–41.
5. Włodarczyk E, Janiszewski J. Dynamiczne stany naprężenia i skończonego odkształcenia w metalowym cienkim pierścieniu rozszerzanym wybuchowo. Biuletyn Wojskowej Akademii Technicznej. 2007;Vol. 56(nr 1):126–42.
6. Clough EC, Plaisted TA, Eckel ZC, Cante K, Hundley JM, Schaedler TA. Elastomeric Microlattice Impact Attenuators. Matter. 2019 Dec;1(6):1519–31.
7. Trzaskalska M, Chwastek R. Damping Properties and Density of Helmet Liners Made of Expanded Polystyrene (EPS). Archives of Metallurgy and Materials. 2021;66(1):339–44.

DOI 10.2478/ama-2024-0035

8. Reyes A, Børvik T. Low velocity impact on crash components with steel skins and polymer foam cores. International Journal of Impact Engineering. 2019 Oct;132:103297.
9. Koohbor B, Blourchian A, Uddin KZ, Youssef G. Characterization of Energy Absorption and Strain Rate Sensitivity of a Novel Elastomeric Polyurea Foam. Adv Eng Mater. 2021 Jan;23(1):2000797.
10. Mizuno K, Ito D, Oida K, Kobayashi G, Han Y. Head protection with cyclist helmet in impact against vehicle A-pillar. International Journal of Crashworthiness. 2017 May 4;22(3):322–31.
11. Raponi E, Fiumarella D. Experimental analysis and numerical optimization of a thermoplastic composite in crashworthiness. IOP Conf Ser: Mater Sci Eng. 2021 Feb 1;1038(1):012030.
12. Kathiresan M, Manisekar K, Manikandan V. Crashworthiness analysis of glass fibre/epoxy laminated thin walled composite conical frusta under axial compression. Composite Structures. 2014 Feb;108:584–99.
13. Tarlochan F. Sandwich Structures for Energy Absorption Applications: A Review. Materials. 2021 Aug 22;14(16):4731.
14. Jabłońska MB, Śmiglewicz A, Niewielski G. The Effect Of Strain Rate On The Mechanical Properties And Microstructure Of The High-Mn Steel After Dynamic Deformation Tests. Archives of Metallurgy and Materials. 2015 Jun 1;60(2):577–80.
15. Stankiewicz M, Popławski A, Bogusz P, Gieleta R, Sławiński G. Experimental Evaluation Of Energy Absorbing Properties Of Selected Elastomer Materials. Journal of KONES Powertrain and Transport. 2015 Jan 1;22(3):241–8.
16. Liang W, Bonsu AO, Tang X, Lei Z, Yang B. Impact and CAI behavior of SGF mat filled sandwich panels made from foam core and FRP facesheet. Composites Communications. 2022 Jan;29:101000.
17. Avalle M, Belingardi G. A Mechanical Model of Cellular Solids for Energy Absorption. Adv Eng Mater. 2019 Apr;21(4):1800457.
18. Sun G, Li G, Hou S, Zhou S, Li W, Li Q. Crashworthiness design for functionally graded foam-filled thin-walled structures. Materials Science and Engineering: A. 2010 Mar;527(7–8):1911–9.
19. Robinson MB, Stousland T, Baqui M, Karami G, Ziejewski M. Reducing effect of softball-to-head impact by incorporating slip-surface in helmet. Procedia Engineering. 2011;13:415–21.
20. Maw S, Lun V, Clarke A. The influence of helmet size and shape on peak linear decelerations when impacting crash pads. Procedia Engineering. 2012;34:819–24.
21. Lewis LM, Naunheim R, Standeven J, Lauryssen C, Richter C, Jeffords B. Do Football Helmets Reduce Acceleration of Impact in Blunt Head Injuries? Acad Emergency Med. 2001 Jun;8(6):604–9.
22. Whyte T, Gibson T, Eager D, Milthorpe B. Response of a full-face motorcycle helmet FE model to the UNECE 22.05 chin bar impact test. International Journal of Crashworthiness. 2016 Nov;21(6):555–65.
23. Ghajari M, Peldschus S, Galvanetto U, Iannucci L. Evaluation of the effective mass of the body for helmet impacts. International Journal of Crashworthiness. 2011 Dec;16(6):621–31.
24. Wu JZ, Pan CS, Ronaghi M, Wimer BM, Reischl U. Application of polyethylene air-bubble cushions to improve the shock absorption performance of Type I construction helmets for repeated impacts. BME. 2021 Jan 21;32(1):1–14.
25. Mazurek K, Szyguła M. Dynamic analysis of thin-walled structures as energy absorbers. MM. 2020 Jul 6;(162):2–12.
26. Böhm R, Hornig A, Weber T, Grüber B, Gude M. Experimental and Numerical Impact Analysis of Automotive Bumper Brackets Made of 2D Triaxially Braided CFRP Composites. Materials. 2020 Aug 12;13(16):3554.

The authors acknowledge Ozygała Marcin Bolesław, the patent owner nr P.421930, title: Osłona ochronna, issued on 2017.06.15 by Patent Office of the Republic of Poland for providing research materials.

Maciej Obst: https://orcid.org/0000-0001-6555-6198

Dariusz Kurpisz: https://orcid.org/0000-0003-2233-8638

Michał Jakubowski: https://orcid.org/0009-0000-7888-1520